Research Article

Original photochemical synthesis of Ag nanoparticles mediated by potato starch

Michele Avila dos Santos[1] · Leonardo Giordano Paterno[1] · Sanclayton Geraldo Carneiro Moreira[2] · Maria José Araújo Sales[1]

Abstract

In this contribution, we report an original photochemical method and its mechanism, in which Ag nanoparticles (AgNPs) are formed in the presence of starch. $AgNO_3$/potato starch aqueous suspensions are irradiated (254 nm, 8 W) at room temperature and the Ag^+/starch ratio can be varied to tune the size of AgNPs. The evolution of the AgNPs plasmon resonance band during the reaction is monitored by UV–Vis spectroscopy and evidences that AgNPs are formed in a two-stage process combining nucleation and growth, with the nucleation being controlled by the amount of added starch. Moreover, infrared and Raman spectra indicates that starch undergoes oxidation simultaneously to Ag^+ reduction, even though starch alone is not capable of reducing Ag^+ at an appreciable rate and UV irradiation is essential to produce sizeable amounts of AgNPs. Transmission electron microscopy reveals that AgNPs are nearly spherical with diameters ranging between 13 and 8 nm. The AgNPs/starch suspensions exhibit hydrodynamic diameters between 150 and 200 nm and zeta potentials very close to zero. Since AgNPs/starch suspensions are very stable over time, the colloidal stability is ensured by the steric hindrance imposed by starch rather than electrostatic repulsion.

Electronic supplementary material The online version of this article (https://doi.org/10.1007/s42452-019-0586-1) contains supplementary material, which is available to authorized users.

✉ Maria José Araújo Sales, mjsales@unb.br | [1]Laboratory of Research on Polymers and Nanomaterials, Institute of Chemistry, University of Brasilia, Brasília, DF 70904-970, Brazil. [2]Institute of Physics, Federal University of Para, Belém, PA, Brazil.

SN Applied Sciences (2019) 1:554 | https://doi.org/10.1007/s42452-019-0586-1

Received: 14 March 2019 / Accepted: 9 May 2019 / Published online: 13 May 2019

Graphical abstract

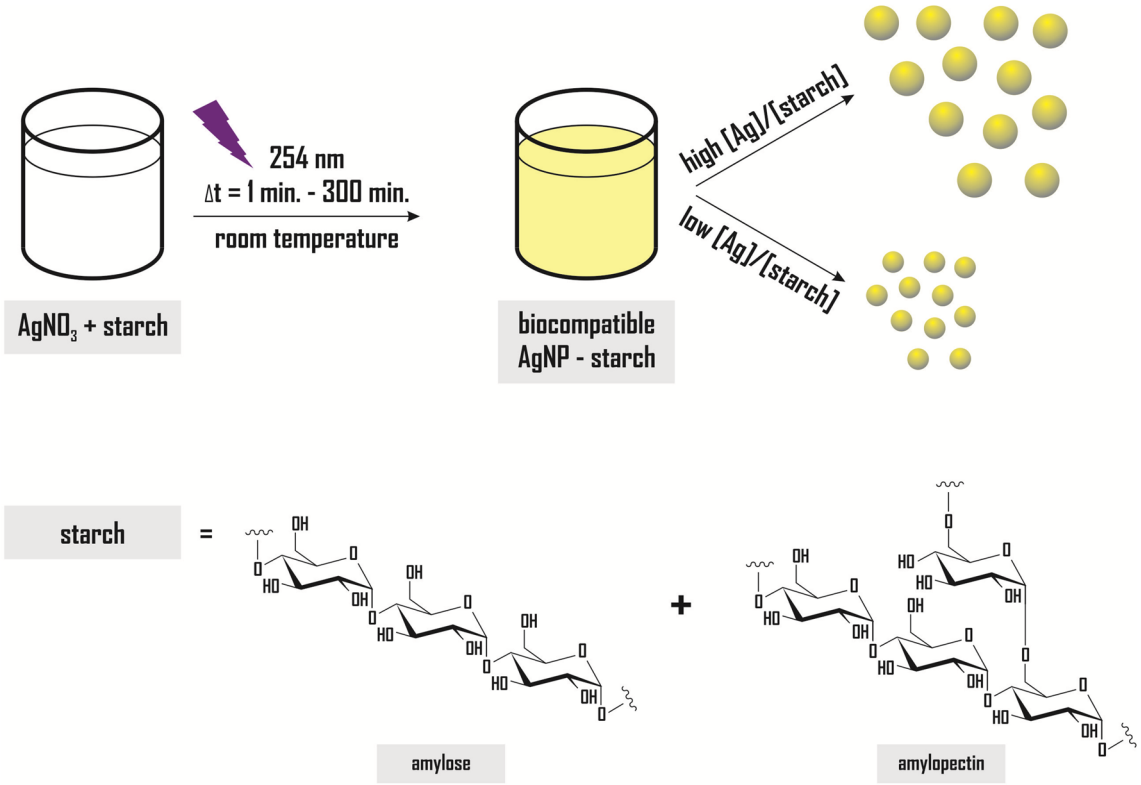

Keywords Silver nanoparticles · Starch · Photochemical synthesis · Photochemical kinetic

1 Introduction

The use of silver nanoparticles (AgNPs) in commercial products has increased in recent years. This demonstrates the importance of research and developing new and inexpensive synthesis methods to allow their mass production and incorporation into the desired product [1, 2]. In addition, it is necessary to understand the mechanisms of these synthetic routes to increase their efficiency. Several routes have been developed with the aim of using natural materials such as starch to coat, protect and stabilize AgNPs [3–5].

Starch is a very promising natural polymer for the development of new technologies because it is renewable, biodegradable, and widely available [6, 7]. In addition, its mechanical, electrical, optical, and thermal properties can be improved further by chemical modifications or combination with nanosized additives, which can diversify and increase its utilization [8–11].

Starch can be employed for the synthesis of AgNPs in order to mitigate the potential harm of common reducing agents and afford green synthetic procedures. These approaches will certainly promote the use of AgNPs in several areas such as microelectronics and biomedicine [3, 12–17]. In addition, to its physical, chemical and biological properties, the commercial availability of AgNPs products has increased at an incredible rate [18], beyond its excellent catalytic property when deposited onto cellulose microfibers [19, 20] and as potential applications in smart windows and anti-counterfeit labels [21]. Also, the combination of colloid silver as filler and chitosan as matrix for the preparation of thin nanocomposite films for functional coating of polymeric stents [22], as well as nanofiber webs of chitosan (CS)/poly(vinyl alcohol) (PVA) blends incorporated with AgNPs showed antibacterial ability against *Escherichia coli* [23]. Recently published researches have shown that the green synthesis for AgNPs coated with natural polymers such as chitosan and pectin have antibacterial activity and, in addition, they demonstrated to be non-cytotoxic for fibroblasts [24, 25]. Moreover, Pallavicini et al. [24] showed that AgNPs coated with pectin can combine different properties such as antibacterial action and wound healing in the same material.

Thus, the AgNPs syntheses at low cost and reduced environmental impact have attracted great interest.

It can be seen that the starch has been effectively used as a stabilizing agent in several AgNPs syntheses, as well as a potential reducing agent [3, 4, 26–31]. Furthermore, the reduction of Ag^+ ions can be photochemically-assisted by UV radiation. The photochemically-assisted method offers one several advantages. It is cleaner, because the UV radiation replaces the reducing agent, and it is faster, because the excited species, $[Ag^+]^*$, generated thereof proceeds faster the reduction of Ag^+ to Ag^0. Moreover, the experimental apparatus is of low cost and allows one for the in situ production of nanoparticles in different media, including, but not limited to emulsions, glasses, and polymer matrices [13]. In conclusion, the association of starch with photoreduction techniques is a promising green route for AgNPs synthesis.

In this study, we propose a kinetic study of a fast, inexpensive, scalable route for industrial production that originally associates starch and UV radiation. While the literature collects several contributions regarding the usage of starch together and other reducing agents or UV radiation in other matrices, herein we use both, simultaneously, to synthesize AgNPs, what has not been investigated so far. Moreover, we have performed a systematic investigation by UV–Vis and micro Raman spectroscopies, transmission electron microscopy (TEM), dynamic light scattering (DLS) and zeta potential measurements from which we are capable to propose a mechanism of AgNPs formation as well as to identify the roles played by starch and the UV radiation.

2 Experimental section

2.1 Materials

Potato starch (Lot: SZBD2670 V) purchased from Sigma-Aldrich and silver nitrate analytical grade from VETEC-Sigma (Brazil) were used as received. All suspensions were prepared with ultrapure water (resistivity: 18 MΩ cm) provided by a Millipore Milli-Q water purification system. All glassware were carefully cleaned with aqua regia solution and then rinsed with plenty of ultrapure water.

2.2 Photochemically-assisted synthesis of AgNPs

In a typical synthesis run, in a small Erlenmeyer flask (250 mL), 0.1 g of starch were suspended in 80 mL of ultrapure water under mechanical stirring (2500 rpm) at 95 °C for 1 h. This process is performed in order to gelatinize starch, in which starch granules are broken in smaller pieces and become more soluble in water. After this time, heating and stirring were turned off and the resulting milky suspension was left at rest until reaching the room temperature (~ 25 °C). The final volume was adjusted to 80 mL again because of eventual water evaporation. The suspension was then equally divided into two aliquots of 40 mL each. The first aliquot was transferred to a 50 mL volumetric flask and the remaining volume completed with ultrapure water, in order to obtain a final starch concentration of 1 g L^{-1}. This is the control starch sample. The second one was transferred to another 50 mL volumetric flask and the volume filled until 50 mL with a proper volume of $AgNO_3$ solution (0.3 mol L^{-1}). The final concentrations of starch and $AgNO_3$ in that suspension were 1 g L^{-1} and 30 mmol L^{-1}, respectively. That suspension was transferred to a beaker (80 mL) and mechanically stirred for more 10 min. In a temperature-controlled room at 20 °C, this beaker was placed inside the UV cabinet and exposed to UV radiation for different periods to produce the AgNPs (Figure S1, supplementary information, provides a schematic view of the synthesis process). The photochemically-assisted synthesis of AgNPs was carried out in a lab-made cabinet comprised by one UV lamp (8 W, 254 nm, Osram) and a computer fan (Figure S2, supplementary information).

2.3 Kinetics of photochemical synthesis

The kinetics of formation of AgNPs was investigated with ex situ UV–Vis spectroscopy by monitoring the localized surface plasmon resonance (LSPR) band of AgNPs in the visible range. In summary, samples were irradiated by different time periods and an UV–Vis spectrum was immediately registered. Different factors were investigated. The first one was to compare the different kinetics of synthesis carried out in the dark, ambient light, and UV irradiation. The suspensions stored in the dark and the exposed to ambient light did not show significant changes even after 400 min of reaction. Then, to verify whether the reaction under these conditions would occur later, the time of this experiment was extended to 192 h (8 days). For the suspension submitted to UV radiation, 400 min were enough and right before they became very turbid.

The effect of different concentrations of starch and $AgNO_3$ in the photochemically assisted synthesis was evaluated in terms of kinetics constants obtained after proper mathematical fitting of the experimental UV–Vis spectroscopy data. The different samples formulations along with their respective preparation conditions are listed in Table 1.

2.4 Samples characterizations

UV–Vis spectra were registered with a Varian Cary 5000 UV–Vis–NIR spectrophotometer (range 200–800 nm; scan

Table 1 Samples formulations and preparation conditions

Sample	Starch (g L^{-1})	$AgNO_3$ (mM)	Factors investigated
S1	1.25	0.03	$AgNO_3$ influence
S2	1.25	1	$AgNO_3$ influence
S3	1.25	3	$AgNO_3$ influence
S4	1.25	10	$AgNO_3$ influence
S5	1.25	30	$AgNO_3$, starch and radiation influence
S6	0.25	30	Starch influence
S7	2.5	30	Starch influence

rate: 10 nm s^{-1}; resolution: 0.05 nm) with quartz cuvettes of 10 mm optical path and two polished windows. Some samples were subjected to micro Raman spectroscopy using the Jobin Ivon micro-Raman spectrometer model T64000, with a laser excitation of 633 nm (range 100–1800 cm^{-1}; laser power: 17 mW; resolution: 1 cm^{-1}). Few drops of samples were deposited onto glass slides and left to dry. The process was repeated more few times to obtain thicker films for acquiring the Raman spectra.

The attenuated total reflectance Fourier transform infrared (ATR-FTIR) spectra were recorded on a Varian 640 spectrophotometer (range 4000–600 cm^{-1}; number of scans: 16; resolution: 4 cm^{-1}). For this analysis, some samples were dried in a vacuum desiccator.

The colloidal state of samples was evaluated by measuring the hydrodynamic diameter (DH) and zeta potential (ζ) with a Zeta Sizer Nano-ZS equipment, Malvern Instruments. Samples were diluted with ultrapure water at the 1:9 v/v and the data presented corresponded to the average of triplicates. DH data were obtained based on the intensity of the light scattering at 25 °C, with scattering angle set at 90° and laser irradiation at 633 nm.

The morphology of AgNPs nanoparticles was assessed by transmission electron microscopy (TEM) using the Jeol JEM-2100 microscope equipped with the Thermo Scientific X-ray Dispersive Energy Spectrometer. The mean diameter of AgNPs was estimated from a logNormal distribution, the latter obtained after measuring the diameter of at least 300 spherical particles per sample with the aid of the ImageJ software.

3 Results and discussion

3.1 The role of starch and UV radiation for the AgNPs synthesis

As it is discussed in different contributions, starch and many sugars exhibit redox potentials lying in the range which Ag^+ is reduced. Nonetheless, the reduction rate achieved with these substances is quite low and sizeable amounts of AgNPs are attained only after several hours of reaction. Moreover, heating is needed to induce the reaction. Ionizing radiation, including UV, provides sufficient energy to carry out Ag^+ reduction and subsequent formation of AgNPs, and, therefore, able to overcome the common drawbacks of conventional chemical reduction. Which is still not clear are the roles played by starch and UV radiation when they are employed together in the synthesis of AgNPs.

Two initial experiments were carried out in an attempt to answer that question. In the first, the role of starch is investigated by comparing the UV–Vis spectra of plain starch suspension (without $AgNO_3$), plain $AgNO_3$ solution, and starch suspension containing $AgNO_3$ after being submitted to UV irradiation by different time periods, up to 30 min. The results are shown in Fig. 1. It can be noted that plain starch (Fig. 1a) undergoes a small oxidation, as detected by the band peaking in 202 nm, which is typical of $\pi \rightarrow \pi^*$ transition in unsaturated carbon compounds. Nonetheless, it remains colorless, as shown by the cuvette pictured in the inset. Meanwhile, plain $AgNO_3$ solution is unaffected by UV irradiation. Its spectra (Fig. 1b) display an intense band peaking at 300 nm, which corresponds to the $n \rightarrow \pi^*$ transition of the N=O group from the nitrate ion. The shape, absorbance, and energy of such a band do not change with the UV irradiation exposure and the solution remains colorless, as shown by the picture in the inset. However, when starch and $AgNO_3$ are mixed together (Fig. 1c), the formation of AgNPs is quite evident. The LSPR band of AgNPs is already perceived in the first minute of UV irradiation, at about 413 nm. This band suggest the presence of spherical particles and correspond to the out-of-plane dipole resonance [32, 33]. In the curves after 3 min of irradiation, another LSPR mode, the out-of-plane quadrupole resonance [33], occurs around 350 nm and the color change of the suspension becomes more evident. As the UV irradiation time elapses, the LSPR band more intense becomes broadens and shifts to 540 nm. This suggests the formation of anisotropic nanoparticles after long times of irradiation. Part of $AgNO_3$ remains unreacted as the electronic transition ascribed to the nitrate ion paired with Ag^+ is still detected.

In the second experiment, $AgNO_3$/starch suspensions were submitted to different illumination conditions, in the dark, ambient light, and UV irradiation. The UV–Vis spectra of these suspensions were registered at different time intervals and the results are shown in Fig. 2.

As it is clear noted, starch alone is not capable of forming AgNPs. For the dark condition (Fig. 2a), UV–Vis spectra do not show any LSPR signal of AgNPs, even after 192 h

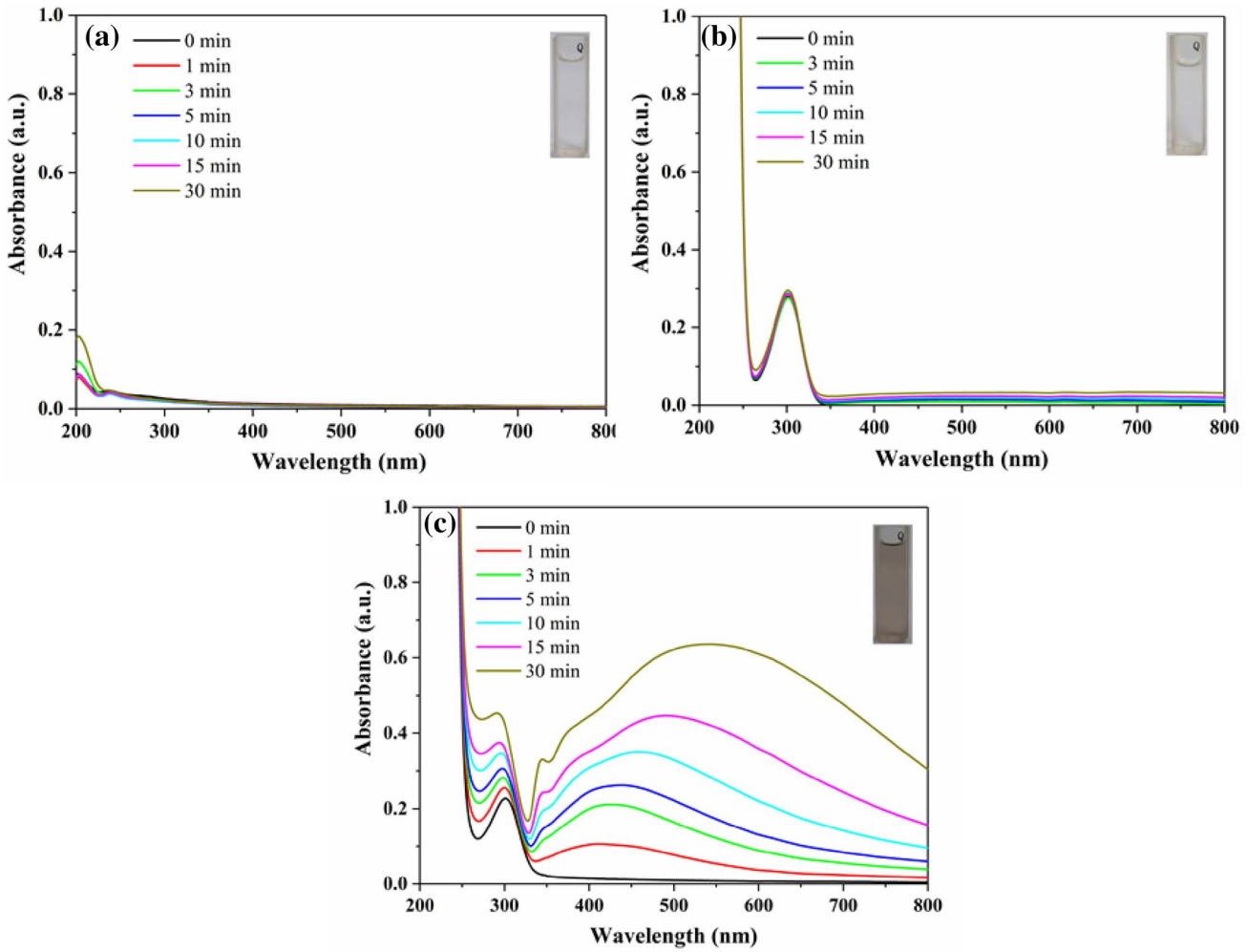

Fig. 1 UV–Vis absorption spectra of **a** plain starch (1 g L^{-1}), **b** plain $AgNO_3$ (30 mM) and **c** starch (1 g L^{-1}) with $AgNO_3$ (30 mM) registered after different exposure times to UV radiation (254 nm). The insets show quartz cuvettes containing respective suspensions after exposed to 10 min of UV irradiation (254 nm)

of reaction. When the suspension is exposed to ambient light, AgNPs are formed since UV–Vis spectra (Fig. 2b) show the LSPR band. Nonetheless, under this condition the photoreduction of Ag^+ is quite slow and the formation of a very low amount of AgNPs takes several hours. Finally, when UV irradiation is employed, the formation of much greater amount of AgNPs is immediate. In fact, with 10 min of UV irradiation, the amount of AgNPs is comparable to that produced after 22 h of reaction under ambient light. This shows that the photochemically-assisted process greatly improves the efficiency of the AgNPs synthesis.

The initial results suggest one that both starch and UV radiation are essential to prepare sizeable amounts of AgNPs in a short period of time reaction. In a previous contribution [34], it was identified the exact roles played by polymer and UV radiation on the photochemically-assisted synthesis of gold nanoparticles (AuNP). It was concluded that while the polymer, in that case polyethylene imine, was responsible only for controlling the nucleation step of AuNP formation, the UV radiation provided the minimum energy (or activation energy) for Au(III) species transform successively into lower redox Au species until zero valence Au. Nonetheless, it was also verified that the polyethylene imine did not suffer any oxidation reaction simultaneously to Au(III) reduction. On the other hand, starch as the assisting polymer can indeed suffer oxidation under the current experimental conditions.

These data suggest that AgNPs formation occurs only in the $AgNO_3$-containing starch suspension after UV irradiation. This synthesis depends crucially on the presence of starch, since the aqueous solution of plain silver nitrate did not show significant changes with the UV irradiation.

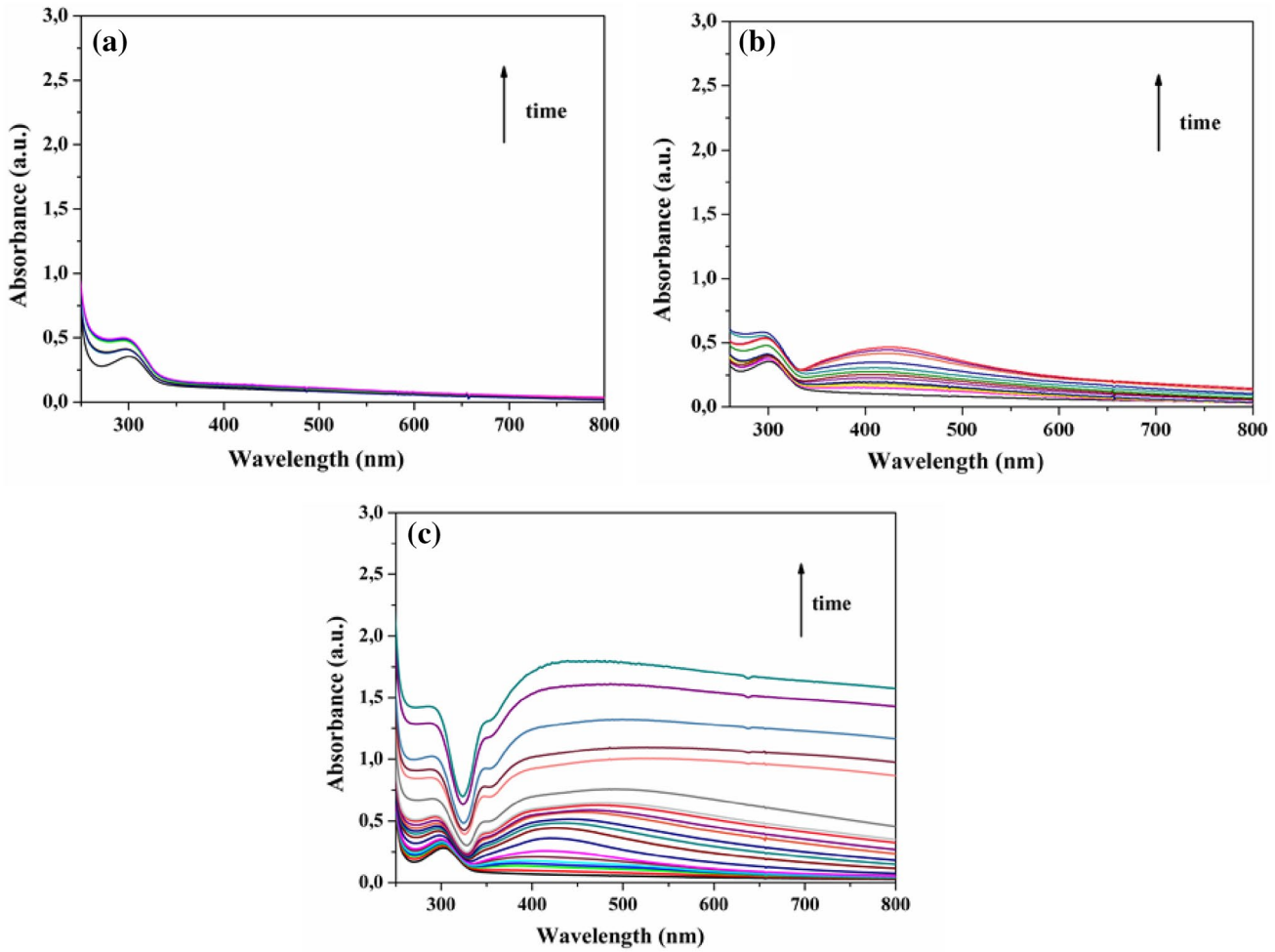

Fig. 2 UV–Vis absorption spectra of the potato starch suspensions (1.25 g L^{-1}) with $AgNO_3$ (30 mM) **a** stored in the dark (0–192 h), **b** exposed to ambient light (0–192 h) and **c** irradiated with UV light (0–400 min)

Figure 3a shows ATR-FTIR spectra of plain starch, starch with $AgNO_3$ unirradiated ($AgNO_3$/starch), after 10 min of UV irradiation (AgNPs/starch) and silver nitrate powder.

The ATR-FTIR spectrum of starch shows characteristics bands at 3352 cm^{-1} for—OH stretching from the aliphatic hydroxyl group, 2933 cm^{-1} for aliphatic C–H stretching and the fingerprint region between 900 and 1200 cm^{-1}. Furthermore, the presence of a weak band at 1648 cm^{-1}, which is ascribed to intermolecular H-bonding involving the carboxyl group, suggests the partial starch oxidation [35]. The effect of the hydrogen bond on the photochemical synthesis of silver nanoparticles was also investigated via experimental and theoretical methods by Zhao et al. [36]. The spectrum of starch with AgNPs show similar features besides very strong bands at 1306 and 803 cm^{-1} related to asymmetric and symmetric modes of N–O stretching of nitrate ions [37]. The intensity of the N–O stretching bands hinders the observation of starch oxidation, the latter being ascribed by the band at 1648 cm^{-1}. In addition, it was noted that the $AgNO_3$/starch suspension reacted during the drying process, probably due to room temperature.

Figure 3b shows the Raman spectra of the $AgNO_3$/starch and AgNPs/starch samples, the latter obtained after 10 min of UV irradiation. This time was sufficient to form AgNPs without causing extensive turbidity. In both spectra, it is possible to observe the signature of starch, with bands in the regions of exocyclic deformations (700 to 500 cm^{-1}) and side group deformations of COH, CCH and OCH groups (950 to 700 cm^{-1} region). Besides that, they exhibit a band at 1040 cm^{-1} that is ascribed to the symmetrical stretching ν_1 of the NO_3^- group of silver nitrate [38, 39]. Nonetheless, as the $AgNO_3$/starch is UV irradiated to become AgNPs/starch, the resulting spectrum is greatly enhanced owing to the SERS effect caused by AgNPs. Moreover, it is possible to perceive a band at 1300 cm^{-1}, which corresponds to carboxyl groups formed after starch oxidation [39]. Along with the UV–Vis and

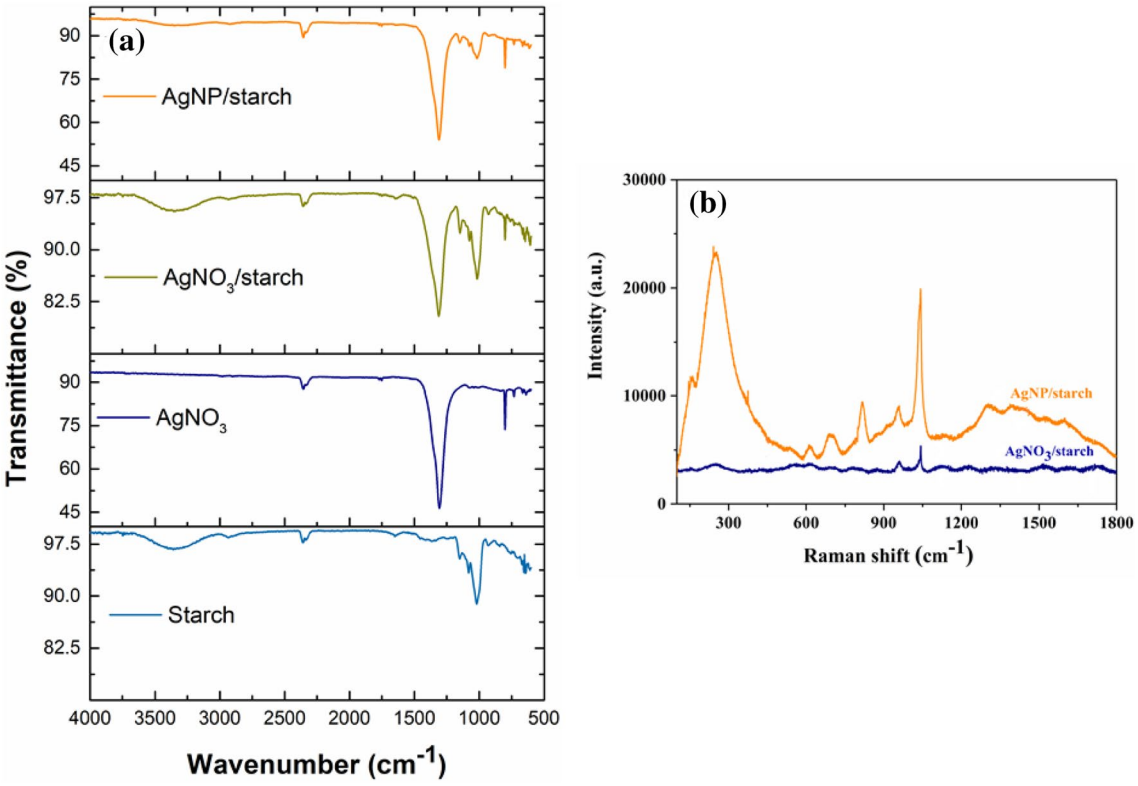

Fig. 3 **a** ATR-FTIR spectra of gelatinized starch, $AgNO_3$/starch, AgNPs/starch and silver nitrate powder; **b** Raman spectra of samples $AgNO_3$/starch and AgNPs/starch. Excitation: 633 nm, laser power: 17 mW

ATR-FTIR analyses presented before, it can be concluded that starch gets oxidized during formation of AgNPs.

3.2 Kinetics of the photochemical synthesis

The kinetics of the photochemical synthesis of AgNPs assisted by starch was investigated varying the concentrations of $AgNO_3$ and starch, independently. The experimental data were further fitted with a two superimposed exponential function, which will be presented and discussed in detail as follows.

Figure 4 provides UV–Vis spectra of $AgNO_3$/starch suspensions registered after they have been submitted to different periods of UV irradiation, for a fixed starch concentration (1.25 g L^{-1}) and different $AgNO_3$ concentrations, as indicated. An increase of the $AgNO_3$ concentration leads to greater amounts of AgNPs, which is consistent with more intense, broader and red-shifted LSPR bands. Broadening and red-shift of the LSPR band are usually ascribed to agglomeration of particles, because the close proximity of particles in a more aggregated state cause distortion of the plasmon waves [40]. On the other hand, Fig. 4 also shows UV–Vis spectra of $AgNO_3$/starch suspensions registered after they have been submitted to different periods of UV irradiation for a fixed $AgNO_3$ concentration (30 mmol L^{-1}) and two different starch concentrations: 0.25 g L^{-1} (Figure S3, supplementary information) and 2.5 g L^{-1}. Similarly, to the effect of $AgNO_3$, as the concentration of starch increases, more AgNPs are formed.

Absorbances at 300 nm, 430 nm, and 500 nm were plotted versus the irradiation time, which is itself the reaction time. In Fig. 4d, e, it is showed the kinetics of the photochemical synthesis using the absorbance at 430 nm versus the irradiation time. This wavelength was chosen because it is where the highest absorbance occurs. Thus, it reflects the behavior of most of the nanoparticles formed. It is important to note that the asymptotic behavior shown in the Fig. 4d, e is common to all samples and wavelengths (Figure S3, supplementary information). This indicates that the equation presented adequately describes the kinetic mechanism of the reaction regardless of the wavelength. That is, even though the wavelength reflects, to a certain extent, the particle size, it is possible by this equation to understand the prevailing phenomena, such as nucleation and growth, by UV–Vis absorption spectroscopy.

For this, different equations with a single exponential term have been applied to fit these data, but all of them were found unsuccessful. Nonetheless, the addition of a second exponential term allowed for a much better fitting, with a coefficient of determination closer to 1 (please refer to

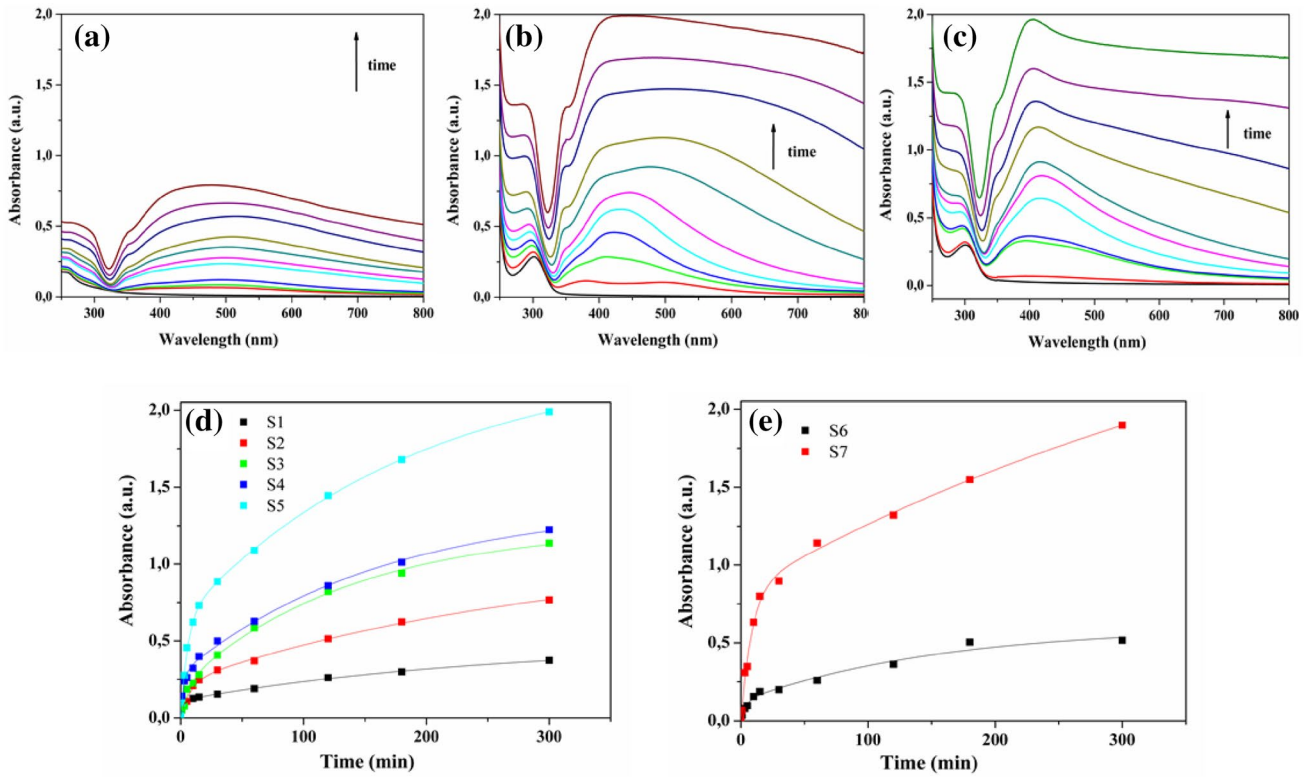

Fig. 4 UV–Vis absorption spectra of suspensions: **a** S2 (1 mM $AgNO_3$, 1.25 g L^{-1}), **b** S5 (30 mM $AgNO_3$, 1.25 g L^{-1}), **c** S7 (30 mM of $AgNO_3$, 2.5 g L^{-1} starch) after 1, 3, 5, 10, 15, 30, 60, 120, 180 e 300 min of UV irradiation, and **d** absorbance curves at 430 nm versus time of exposure to UV radiation from S1, S2, S3, S4 and S5, and **e** from S6 and S7

Table S1, supplementary information). The mentioned equation is given as follows:

$$A = A_0 + k_1\left[1 - \exp\left(\frac{t}{\tau_1}\right)\right] + k_2\left[1 - \exp\left(\frac{t}{\tau_2}\right)\right] \quad (1)$$

in which A and A_0 are the absorbances (in arbitrary units) measured at any time t (in min.) and t = 0, respectively, k_1 and k_2 are, respectively, the nucleation and growth rate constants (in min^{-1}), and τ_1 and τ_2 stand for the process time constant (in min). The first exponential term of Eq. 1 corresponds to the nanoparticles' nucleation while the second one refers to the nanoparticles' growth. Equation 1 is closely related to the Johnson–Mehl–Avrami–Kolmogorov equation except by the absence of the constant "n" (Avrami constant) in the second exponential, originally written as $1 - \exp(t/\tau_2)^n$. The Avrami constant n stands for the growth dimension of particles. For example, if n assumes integer values, when n = 1 one should expect for rod-shaped particles, while for n = 2 and n = 3, it is expected for disk-shaped and spherical particles, respectively. For irregular shapes, n may assume non-integer values. In our approach, n could be set equal as 1. Nonetheless, as it will be seen, AgNPs photochemically synthesized in the presence of starch are nearly spherical for all reaction compositions tested herein.

Table S1 (supplementary information) describes values of k_1, k_2, τ_1, and τ_2 determined after fitting data in the graphs of the absorbance at 300 nm, 430 nm and 500 nm against the irradiation time obtained by Eq. 1 in the Origin 8.0 software. As it can be noted, fitting is quite good for all the wavelengths probed except for sample S6 (with R^2 around 0.97). Additionally, the rate constant and characteristic irradiation time as function of $AgNO_3$ and starch concentrations, collected at 430 nm, are displayed in Fig. 5, because this wavelength represents most of the nanoparticles formed. The rate constant k_1, which stands for the nucleation step of AgNPs formation, reaches a maximum at $[AgNO_3] = 3$ mmol L^{-1} and then decreases at higher $AgNO_3$ concentrations. Simultaneously, k_1 increases with the concentration of starch, which suggests one that starch acts more on the nucleation step of AgNPs formation. Meanwhile, k_2, which stands for the nanoparticles' growth rate, shows a sigmoidal dependence with $[AgNO_3]$ and reaches a maximum at [starch] = 1.25 g L^{-1}. The sigmoidal behavior is typical of induced processes, in which the growth starts when a minimum number of nuclei of the new phase, AgNPs, is formed. The time constants,

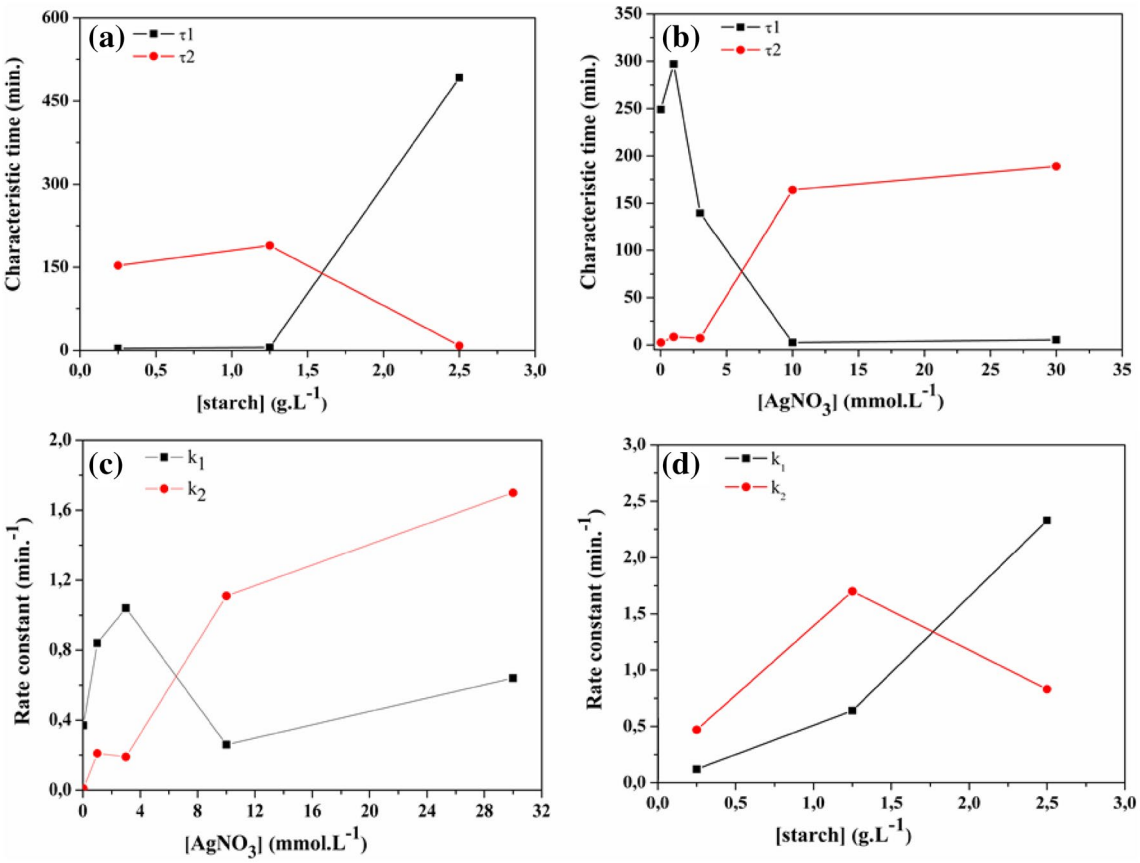

Fig. 5 Rate constant and characteristic time as a function of $AgNO_3$ and starch concentrations

τ_1 and τ_2, can be taken as inversely proportional to the radial velocity of the particles' growth. In fact, rate constants k_1 and k_2 are proportional to τ_1 and τ_2. Since k_1 and τ_1 increase with the starch concentration, starch can be regarded as responsible for the nanoparticles' nucleation. Therefore, one should expect that the AgNPs sizes diminish as the starch concentration increases. This hypothesis is confirmed by TEM micrographs and the AgNPs diameters calculated from it (see Fig. 6). On the other hand, k_2 and τ_2 increase with the concentration of $AgNO_3$. Since these terms are regarded to nanoparticle's growth, the rate of growth should increase with the concentration of $AgNO_3$ simply because more Ag^+ will be available in the reaction medium. However, since the nucleation step is controlled by the starch concentration, for a fixed starch concentration one should not expect for changes in AgNPs sizes as influenced by the $AgNO_3$ concentration. Again, nanoparticles diameters calculated from TEM micrographs confirm this hypothesis as well. Therefore, it can be safely concluded that starch plays a major role on the nucleation step of AgNPs formation.

According to the data obtained by this kinetics study and the characterization by UV-Vis spectroscopy, it is considered that to obtain smaller and more uniform particles the optimal UV irradiation time is between 5 and 15 min. In addition, samples S5 and S7 presented relatively narrower and intense UV–Vis absorption curves, with the LSPR band close to 430 nm, which suggests one the formation of smaller and more uniform particles. Therefore, 10 min of UV irradiation seems to be the optimal condition for preparation of uniform and small AgNPs.

3.3 Suspensions characterization

Another important aspect to be evaluated is the stabilization of nanoparticles. Then, S2, S5, and S7 were selected to verify the suspension stability after UV irradiation is ceased. S5 and S7 were chosen because of their strong absorption and narrower bands, especially when irradiated for 10 min. On the other hand, S2 was selected for comparative purposes, because it behaved differently from the first two after being irradiated by the same time. It is likely that S2 sample is highly polydisperse. Samples were irradiated for 10 min and UV–Vis spectra were registered afterwards at different elapsed times, for a period of 19 days. During the entire experiment, samples were

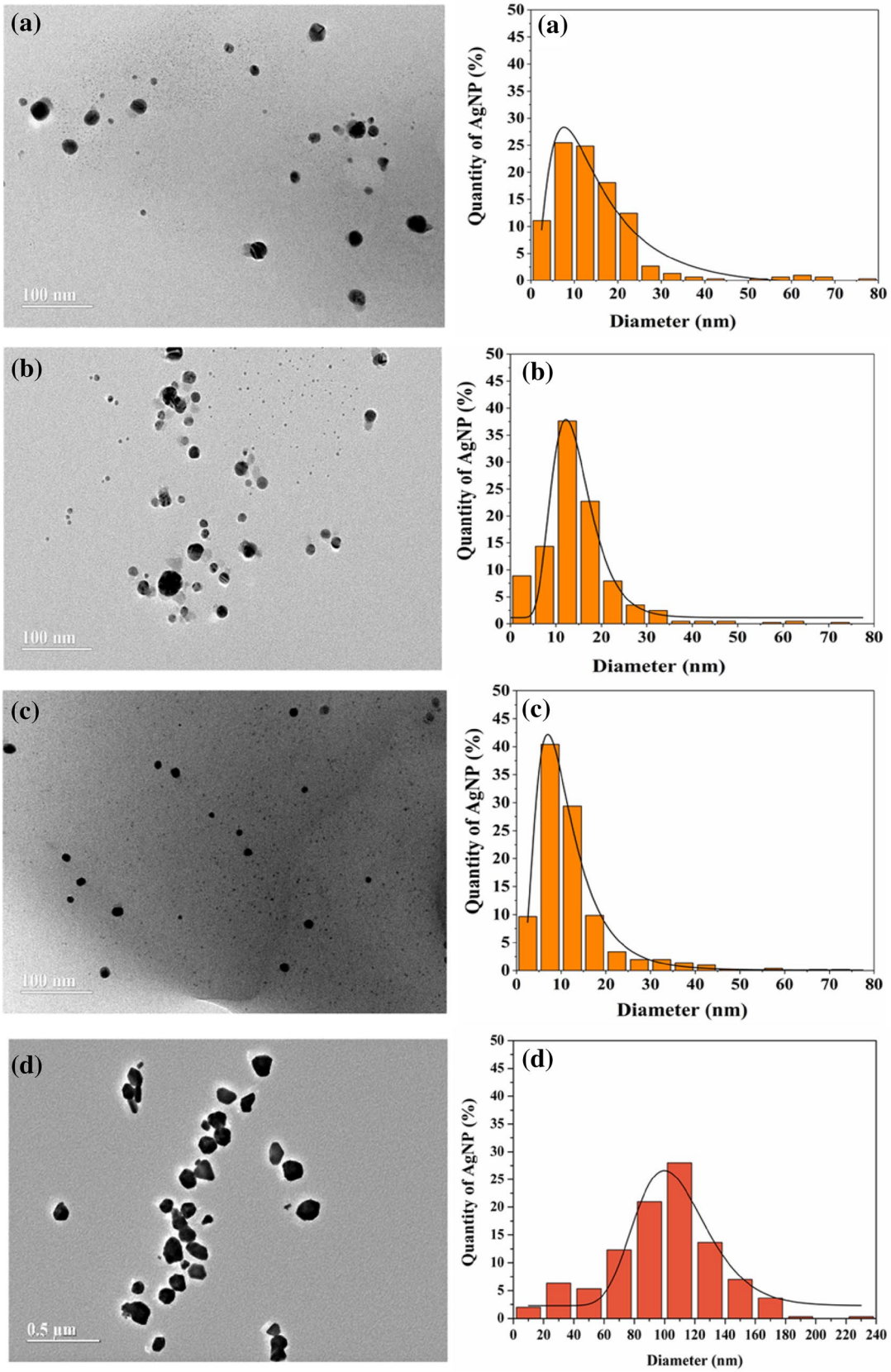

Fig. 6 TEM micrographs of the samples **a** S2, **b** S5, **c** S7 irradiated for 10 min after the 19 days of storage and **d** S5 irradiated for 300 min with their respective size distribution charts

Table 2 Colloidal and morphological features of photochemically synthesized AgNPs

Sample	Zeta potential (mV)	Hydrodynamic diameter (nm)	TEM diameter (nm)
S2	−10.9 ± 3.82	148.2 ± 36.46	13.8 ± 0.7
S5	−2.1 ± 3.37	200.3 ± 51.81	13.7 ± 0.3
S7	−2.7 ± 4.08	174.1 ± 70.17	9.8 ± 0.5

stored and protected from light, although exposed to environmental climatic variations. During this period, the average maximum temperature was 30 °C and the average minimum temperature was 19 °C. The results are collected in Figure S4, supplementary information.

As it can be noted, all the three samples undergo some change during the 19 days of observation. The most critical is seen with sample S2. Right after UV irradiation is ceased (t = 0), its spectrum is broad and displays two main absorptions; a stronger one at 500 nm and a weaker one below 400 nm. As the time elapses, these two bands gradually merge into a single one peaking at 430 nm. It was also noted that S2 acquired a slightly yellowish coloration over time. This behavior suggests that not all $AgNO_3$ reacted during the time frame of the UV irradiation and, possibly, reduction of Ag^+ to metallic Ag keeps going on even after that. This observation is in support to the hypothesis that starch reduces Ag^+ ions. The same is true for samples S5 and S7 or else, the $Ag^+ \rightarrow Ag^0$ conversion continues even after the UV irradiation is ceased, since the maximum absorbance keeps increasing. Nonetheless, the shape of the LSPR band remains the same as well as the location of λ_{max}.

The zeta potential, hydrodynamic diameter and mean diameter obtained by TEM of samples S2, S5 and S7 were determined after the 19 days of storage and are listed in Table 2. The zeta potentials are relatively low, which rules out electrostatic stability of AgNPs/starch suspensions and suggests the stability is mainly due to steric hindering as caused by starch chains. It was also observed that, after increasing the $AgNO_3$ concentration, the modulus of zeta potential decreases (not shown), probably due to the presence of remaining Ag^+ cations. On the other hand, the increase of the starch concentration did not cause a significant modification on the zeta potential. Hydrodynamic diameters are considerably high and much greater than mean diameters determined by TEM. This is consistent with the starch coating AgNPs.

TEM micrographs of samples S2, S5, and S7 along with size distributions are provided in Fig. 6. In all the three samples, AgNPs are nearly spherical, with a mean diameter ranging from 13 to 8 nm, as shown in Table 2. The similar sizes of S2 and S5 can be attributed to the exposure to the environmental climatic conditions for 19 days. In addition, the distribution profile in Fig. 6 confirms that S2 has a higher polydispersity as suggested by UV–Vis spectra shown in Figure S4, supplementary information. In addition, Fig. 6d shows that longer exposure to UV irradiation promotes the formation of NP of different sizes and shapes. In fact, after 300 min of UV irradiation the D_{TEM} is over 100 nm, which is about 8 times greater than that achieved after 10 min of irradiation. Thus, it is believed that the grayish coloration and high turbidity, obtained after long UV exposure times, can be attributed to the agglomeration of the AgNPs.

4 Conclusions

Silver nanoparticles (AgNPs) were prepared by a photochemical method in the presence of potato starch, which allows the fast and inexpensive production of nanoparticles. It was verified that the presence of starch combined with UV irradiation is essential for the preparation of sizeable amounts of AgNPs. In addition it was possible to describe the kinetic mechanism for this synthetic route, which allows for a better control of the synthesis and increase the process efficiency. According to the reaction kinetics assessed by UV–Vis spectroscopy, starch plays the role of nucleating agent while dynamic light scattering and zeta potential measurements points starch as a stabilizer as well. AgNPs prepared under the photochemical approach were nearly spherical, with diameters being modulated by the Ag^+/starch ratio. Since starch is cheap and readily available, and the experimental set-up for the photochemical synthesis is easily assembled, the method proposed herein is highly promising for the accessible and of low cost production of AgNPs. It is worth mentioning that the synthesis used in this work is totally photochemical and, therefore, much simpler and cleaner.

Acknowledgements The authors acknowledge the financial support of Brazilian funding agencies CNPq (Process No. 308038/2012-6), CAPES/Pró-Amazônia (Process No. 3333-047/2012), and FAP-DF (Process No. 0193.000829/2015).

Compliance with ethical standards

Conflict of interest The authors declare that they have no conflict of interest.

References

1. Zhang H, Zou G, Liu L, Tong H, Li Y, Bai H, Wu A (2017) Synthesis of silver nanoparticles using large-area arc discharge and

its application in electronic packaging. J Mater Sci 52(6):3375–3387. https://doi.org/10.1007/s10853-016-0626-9
2. Gong H, Liu M, Li H (2019) In situ green preparation of silver nanoparticles/chemical pulp fiber composites with excellent catalytic performance. J Mater Sci 54(9):6895–6907. https://doi.org/10.1007/s10853-018-03205-w
3. Vasileva P, Donkova B, Karadjova I, Dushkina C (2011) Synthesis of starch-stabilized silver nanoparticles and their application as a surface plasmon resonance-based sensor of hydrogen peroxide. Colloids Surf A Physicochem Eng Asp 382:203–210. https://doi.org/10.1016/j.colsurfa.2010.11.060
4. Vasileva P, Alexandrova T, Karadjova I (2017) Application of starch-stabilized silver nanoparticles as a colorimetric sensor for mercury (II) in 0.005 mol/L nitric acid. J Chem 2017:1–9. https://doi.org/10.1155/2017/6897960
5. Sun L, Lv P, Li H, Wang F, Su W, Zhang L (2018) One-stepsynthesis of Au–Ag alloy nanoparticles using soluble starch and their photocatalytic performance for 4-nitrophenol degradation. J Mater Sci 53:15895–15906. https://doi.org/10.1007/s10853-018-2763-9
6. Paraginski RT, Vanier NL, Moomand K, de Oliveira M, Zavareze ER, Silva RM, Ferreira CD, Cardoso ME (2014) Characteristics of starch isolated from maize as a function of grain storage temperature. Carbohydr Polym 102:88–94. https://doi.org/10.1016/j.carbpol.2013.11.019
7. Waterschoot J, Gomand SV, Fierens E, Delcour JA (2015) Production, structure, physicochemical and functional properties of maize, cassava, wheat, potato and rice starches. Starch-Stärke 67(1–2):14–29. https://doi.org/10.1002/star.201300238
8. Masina N, Choonara YE, Kumar P, du Toit LC, Govender M, Indermun S, Pillay V (2017) A review of the chemical modification techniques of starch. Carbohydr Polym 157:1226–1236. https://doi.org/10.1016/j.carbpol.2016.09.094
9. Peregrino PP, Sales MJA, da Silva MFP, Soler MAG, da Silva LFL, Moreira SGC, Paterno LG (2014) Thermal and electrical properties of starch–graphene oxide nanocomposites improved by photochemical treatment. Carbohydr Polym 106:305–311. https://doi.org/10.1016/j.carbpol.2014.02.008
10. Xie F, Pollet E, Halley PJ, Avérous L (2013) Starch-based nanobiocomposites. Prog Polym Sci 38(10–11):1590–1628. https://doi.org/10.1016/j.progpolymsci.2013.05.002
11. Cheviron P, Gouanvé F, Espuche E (2015) Effect of silver nanoparticles' generation routes on the morphology, oxygen, and water transport properties of starch nanocomposite films. J Nanopart Res 17(364):1–16. https://doi.org/10.1007/s11051-015-3173-4
12. Abou El-Nour KMM, Eftaiha A, Al-Warthan A, Ammar RAA (2010) Synthesis and applications of silver nanoparticles. Arab J Chem 3(3):135–140. https://doi.org/10.1016/j.arabjc.2010.04.008
13. Sakamoto M, Fujistuka M, Majima T (2009) Light as a construction tool of metal nanoparticles: synthesis and mechanism. J Photochem Photobiol C 10(1):33–56. https://doi.org/10.1016/j.jphotochemrev.2008.11.002
14. Sharma VK, Yngard RA, Lin Y (2009) Silver nanoparticles: green synthesis and their antimicrobial activities. Adv Colloid Interface Sci 145(1–2):83–96. https://doi.org/10.1016/j.cis.2008.09.002
15. Ahmed S, Ahmad M, Swami BL, Ikram S (2016) A review on plants extract mediated synthesis of silver nanoparticles for antimicrobial applications: a green expertise. J Adv Res 7:17–28. https://doi.org/10.1016/j.jare.2015.02.007
16. Vigneshwaran N, Nachane RP, Balasubramanya RH, Varadarajan PV (2006) A novel one-pot 'green' synthesis of stable silver nanoparticles using soluble starch. Carbohydr Res 341(12):2012–2018. https://doi.org/10.1016/j.carres.2006.04.042
17. Oluwafemi OS, Vuyelwa N, Scriba M, Songca SP (2013) Green controlled synthesis of monodispersed, stable and smaller sized starch-capped silver nanoparticles. Mater Lett 106:332–336. https://doi.org/10.1016/j.matlet.2013.05.001
18. Vance ME, Kuiken T, Vejerano EP, McGinnis SP, Hochella MF, Hull DR (2015) Nanotechnology in the real world: redeveloping the nanomaterial consumer products inventory. Beilstein J Nanotechnol 6(1):1769–1780. https://doi.org/10.3762/bjnano.6.181
19. Xu P, Cen C, Chen N, Lin H, Wanga Q, Xu N, Tang J, Teng Z (2018) Facile fabrication of silver nanoparticles deposited cellulose microfiber nanocomposites for catalytic application. J Colloid Interface Sci 526:194–200. https://doi.org/10.1016/j.jcis.2018.04.045
20. Liang M, Zhang G, Feng Y, Li R, Hou P, Zhang J, Wang J (2018) Facile synthesis of silver nanoparticles on amino-modified cellulose paper and their catalytic properties. J Mater Sci 53(2):1568–1579. https://doi.org/10.1007/s10853-017-1610-8
21. Liu L, Wang L, Luo S, Qing Y, Yan N, Wu Y (2019) Chiral nematic assemblies of silver nanoparticles in cellulose nanocrystal membrane with tunable optical properties. J Mater Sci 54(8):6699–6708. https://doi.org/10.1007/s10853-019-03321-1
22. Pakseresht S, Alogaili AWM, Akbulut H, Placha D, Pazdziora E, Klushina D, Konvicková Z, Kratošová G, Holešová S, Martynková GS (2019) Silver/chitosan antimicrobial nanocomposites coating for medical devices: comparison of nanofiller effect prepared via chemical reduction and biosynthesis. J Nanosci Nanotechnol 19(5):2938–2942. https://doi.org/10.1166/jnn.2019.15863
23. Nguyen TTT, Tae B, Park JS (2011) Synthesis and characterization of nanofiber webs of chitosan/poly(vinyl alcohol) blends incorporated with silver nanoparticles. J Mater Sci 46(20):6528–6537. https://doi.org/10.1007/s10853-011-5599-0
24. Pallavicini P, Arciola CR, Bertoglio F, Curtosi S, Dacarro G, D'Agostino A, Ferrari F, Merli D, Milanese C, Rossi S, Taglietti A, Tenci M, Visai L (2017) Silver nanoparticles synthesized and coated with pectin: an ideal compromise for anti-bacterial and anti-biofilm action combined with wound-healing properties. J Colloid Interface Sci 498:271–281. https://doi.org/10.1016/j.jcis.2017.03.062
25. Shao J, Wang B, Li J, Jansen JA, Walboomers XF, Yang F (2019) Antibacterial effect and wound healing ability of silver nanoparticles incorporation into chitosan-based nanofibrous membranes. Mater Sci Eng C 98:1053–1063. https://doi.org/10.1016/j.msec.2019.01.073
26. Bashir O, Khan Z (2014) Silver nano-disks: synthesis, encapsulation, and role of water soluble starch. J Mol Liq 199:524–529. https://doi.org/10.1016/j.molliq.2014.09.041
27. Cheng F, Betts JW, Kelly SM, Hector AL (2015) Green synthesis of highly concentrated aqueous colloidal solutions of large starch-stabilised silver nanoplatelets. Mater Sci Eng C 46:530–537. https://doi.org/10.1016/j.msec.2014.10.041
28. Cheviron P, Gouanvé F, Espuche E (2014) Green synthesis of colloid silver nanoparticles and resulting biodegradable starch/silver nanocomposites. Carbohydr Polym 108(1):291–298. https://doi.org/10.1016/j.carbpol.2014.02.059
29. El-Sheikh MA (2014) A novel photosynthesis of carboxymethyl starch-stabilized silver nanoparticles. Sci World J 2014:1–11. https://doi.org/10.1155/2014/514563
30. Khan Z, Singh T, Hussain JI, Obaid AY, Al-Thabaiti SA, El-Mossalamy EH (2013) Starch-directed green synthesis, characterization and morphology of silver nanoparticles. Colloids Surf B Biointerfaces 102:578–584. https://doi.org/10.1016/j.colsurfb.2012.08.057
31. Velmurugan P, Park JH, Lee SM, Jang JS, Yi YJ, Han SS, Lee SH, Cho KM, Cho M, Oh BT (2015) Reduction of silver (I) using defatted cashew nut shell starch and its structural comparison with commercial product. Carbohydr Polym 133:39–45. https://doi.org/10.1016/j.carbpol.2015.06.097

32. Ledwith DM, Whelan AM, Kelly JM (2007) A rapid, straight-forward method for controlling the morphology of stable silver nanoparticles. J Mater Chem 17:2459–2464
33. D'Agostino A, Taglietti A, Desando R, Bini M, Patrini M, Dacarro G, Cucca L, Pallavicini P, Grisoli P (2017) Bulk surfaces coated with triangular silver nanoplates: antibacterial action based on silver release and photo-thermal effect. Nanomaterials 7(7):1–16. https://doi.org/10.3390/nano7010007
34. Teixeira PR, Santos MSC, Silva ALG, Báo SN, Azevedo RB, Sales MJA, Paterno LG (2016) Photochemically-assisted synthesis of non-toxic and biocompatible gold nanoparticles. Colloids Surf B Biointerfaces 148:317–323. https://doi.org/10.1016/j.colsurfb.2016.09.002
35. Kumar B, Smita K, Cumbal L, Debut A, Pathak R (2014) Sonochemical synthesis of silver nanoparticles using starch: a comparison. Bioinorg Chem Appl 2014:1–8. https://doi.org/10.1155/2014/784268
36. Zhao FJ, Liu L, Yang Y, Zhang RL, Ren GH, Xu DL, Zhou PW, Han KL (2015) Effect of the hydrogen bond on photochemical synthesis of silvernanoparticles. J Phys Chem A 119:12579–12585. https://doi.org/10.1021/acs.jpca.5b09949
37. Miller FA, Wilkins CH (1952) Infrared spectra and characteristic frequencies of inorganic ions. Anal Chem 24(8):1253–1294. https://doi.org/10.1021/ac60068a007
38. Mrozek MF, Weaver MJ (2002) Detection and identification of aqueous saccharides by using surface-enhanced Raman spectroscopy. Anal Chem 74(16):4069–4075. https://doi.org/10.1021/ac020115g
39. Ortega-Arroyo L, Martin-Martinez ES, Aguilar-Mendez MA, Cruz-Orea A, Hernandez-Pérez I, Glorieux C (2013) Green synthesis method of silver nanoparticles using starch as capping agent applied the methodology of surface response. Starch-Stärke 65(9–10):814–821. https://doi.org/10.1002/star.201200255
40. Noguez C (2007) Surface plasmons on metal nanoparticles: the influence of shape and physical environment. J Phys Chem C 111:3806–3819. https://doi.org/10.1021/jp066539m